Title

Novel technique for characterizing prostate cancer utilizing MRI restriction spectrum imaging: proof of principle and initial clinical experience with extraprostatic extension

Journal

Prostate Cancer and Prostatic Diseases, 18(1)

ISSN

1365-7852

Authors

Rakow-Penner, RA
White, NS
Parsons, JK
et al.

Publication Date

2015-03-01

DOI

10.1038/pcan.2014.50

Peer reviewed

Prostate Cancer and Prostatic Disease (2015) 18, 81–85

www.nature.com/pcan

ORIGINAL ARTICLE

Novel technique for characterizing prostate cancer utilizing MRI restriction spectrum imaging: proof of principle and initial clinical experience with extraprostatic extension

RA Rakow-Penner[1], NS White[1], JK Parsons[2], HW Choi[1], MA Liss[2], JM Kuperman[1], N Schenker-Ahmed[1], H Bartsch[1], RF Mattrey[1], WG Bradley[1], A Shabaik[3], J Huang[4], DJA Margolis[5], SS Raman[5], L Marks[6], CJ Kane[2], RE Reiter[6], DS Karow[1] and AM Dale[1]

BACKGROUND: Standard magnetic resonance imaging (MRI) of the prostate lacks sensitivity in the diagnosis and staging of prostate cancer (PCa). To improve the operating characteristics of prostate MRI in the detection and characterization of PCa, we developed a novel, enhanced MRI diffusion technique using restriction spectrum imaging (RSI-MRI).
METHODS: We compared the efficacy of our novel RSI-MRI technique with standard MRI for detecting extraprostatic extension (EPE) among 28 PCa patients who underwent MRI and RSI-MRI prior to radical prostatectomy, 10 with histologically proven pT3 disease. RSI cellularity maps isolating the restricted isotropic water fraction were reconstructed based on all *b*-values and then standardized across the sample with *z*-score maps. Distortion correction of the RSI maps was performed using the alternating phase-encode technique.
RESULTS: 27 patients were evaluated, excluding one patient where distortion could not be performed. Preoperative standard MRI correctly identified extraprostatic the extension in two of the nine pT3 (22%) patients, whereas RSI-MRI identified EPE in eight of nine (89%) patients. RSI-MRI correctly identified pT2 disease in the remaining 18 patients.
CONCLUSIONS: In this proof of principle study, we conclude that our novel RSI-MRI technology is feasible and shows promise for substantially improving PCa imaging. Further translational studies of prostate RSI-MRI in the diagnosis and staging of PCa are indicated.

Prostate Cancer and Prostatic Disease (2015) **18,** 81–85; doi:10.1038/pcan.2014.50; published online 6 January 2015

INTRODUCTION

Multiparametric magnetic resonance imaging (MRI) is an emerging diagnostic tool for the screening, staging and treatment of prostate cancer (PCa).[1–17] However, prostate MRI demonstrates variable sensitivity (49–88%) and specificity (84–89%), which currently limits its clinical utility.[2,3,14]

Standard diffusion-weighted imaging (DWI) improves the operating characteristics of prostate MRI.[2,3,14,16,18,19] DWI detects the diffusivity of microscopic water and subsequently reflects the cellularity and integrity of cells imaged. When combined with T2-weighted imaging and dynamic contrast-enhanced imaging, DWI improves sensitivity and specificity of PCa diagnosis by increasing tumor conspicuity.[2,14,16,18,19]

DWI also suffers from distortion due to magnetic field inhomogeneity[20] and relatively high false-positive rates owing to hemorrhage (for example, from prior biopsy), inflammatory processes and benign nodules in the transitional zone.[21] In order to overcome these challenges and improve magnetic resonance detection of PCa, we have developed a novel, sophisticated diffusion method termed prostate restriction spectrum imaging (RSI) or RSI-MRI.[22,23] By collecting a broader, more extended spectrum of diffusion images,[22] combined with sophisticated modeling of differential water compartments in tissue and correction of spatial distortion,[24] RSI-MRI theoretically focuses on the signal emanating from the intracellular water compartment of tumor cells and thereby minimizes false-positive signals.[25] A similar RSI technique, recently applied to brain imaging, enhanced the signal of glioblastoma multiforme tumors by 10-fold.[23]

In this pilot clinical study, we determined the clinical utility of our novel prostate RSI-MRI technique to stage PCa by assessing the accuracy of RSI-MRI to detect extraprostatic extension (EPE) of tumor.

MATERIALS AND METHODS

Restriction spectrum imaging

In this institutional review board approved study, 28 patients underwent standard T2, perfusion (with Gadolinium) and diffusion protocols at 3 T (Siemens, Erlangen, Germany) with an endorectal coil (Table 1). All imaging was performed at a single institute. The 28 patients had biopsy-proven PCa and an MRI was performed for presurgical planning. The restriction spectrum protocol parameters included *b*-values 0, 800, 1500 and 4000 s mm^{-2} in 30 unique diffusion directions for each nonzero *b*-value. RSI cellularity maps isolating the restricted isotropic water fraction[22] were reconstructed based on all *b*-values, and then standardized across the sample with *z*-score maps. The *z*-score maps were calculated by (i) measuring the mean and s.d. of normal prostate signal from the raw RSI

[1]Department of Radiology, School of Medicine, University of California San Diego, La Jolla, CA, USA; [2]Department of Urology, School of Medicine, University of California San Diego, La Jolla, CA, USA; [3]Department of Pathology, School of Medicine, University of California San Diego, La Jolla, CA, USA; [4]Department of Pathology, David Geffen School of Medicine, University of California Los Angeles, Los Angeles, CA, USA; [5]Department of Radiology, David Geffen School of Medicine, University of California Los Angeles, Los Angeles, CA, USA and [6]Department of Urology, David Geffen School of Medicine, University of California Los Angeles, Los Angeles, CA, USA. Correspondence: Dr DS Karow, Multimodal Imaging Laboratory, Department of Radiology, School of Medicine, University of California, San Diego, 8950 Villa La Jolla Drive Suite C101, La Jolla, 92037, CA, USA. E-mail: dskarow@ucsd.edu
Received 30 July 2014; revised 21 October 2014; accepted 25 October 2014; published online 6 January 2015

Table 1. MRI scan parameters for prostate MRI protocol at 3 T

Pulse sequence	*Parameters*
T2	Axial 3D TSE T2 (Siemens SPACE, TR/TE 3800-5040/101 ETL 13, 14 cm FOV, 256 × 256 matrix, 1.5 mm contiguous slices)
Diffusion-weighted (standard)	Echo planar, TR/TE 3900/60, 21 x 26 cm FOV, 130 × 160 matrix, 3.6 mm slices, 4 NEX, *b*-values 0, 100, 400 and 800 s mm^{-2}
T1 dynamic perfusion imaging	Siemens TWIST, TR/TE 3.9/1.4 ms, 12° flip angle, 26 × 26 cm FOV, 160 × 160 matrix, 3.6 mm slices, 4.75 s per acquisition over 6 min with 15 s injection delay, image analysis using iCAD Versavue
Restriction spectrum imaging	Spin echo EPI, TR/TE 5500/137, 26 × 26 cm FOV, 128 × 96 matrix, 3.6 mm slices, 30 directions at each *b*-value, *b*-values 0, 800, 1500 and 4000 s mm^{-2}.

Abbreviation: EPI, Echo planar imaging; FOV, field of view; MRI, magnetic resonance imaging; NEX, number of excitations.

Table 2. Radiologic findings—documented diagnostic interpretations in nine patients with biopsy-proven localized prostate cancer

Case	*Location*	*Axial clock face location*	*Capsular involvement*	*Technical quality*
1	Right peripheral gland	7–8 o'clock	Focal EPE may involve adjacent right neurovascular bundle. Right seminal vesicle invasion.	Excellent, no limitations
2	Right central peripheral basal mid gland	7 o'clock	Intact, no suspicion for involvement	Excellent, no limitations
3	Right peripheral basal mid gland	8 o'clock	Bulges the capsule with a broad base of contact, organ confined disease	Excellent, no limitations
4	Right peripheral gland lesion	6–9 o'clock	Bulges the capsule, suspicious but not definitive for extracapsular extension	Excellent, no limitations
5	Right peripheral gland from apex to base	5–10 o' clock	Blurring and irregularity of right capsule, suspicious for capsular involvement	Limited spectral quality, does not diminish diagnostic confidence
6	Right peripheral base lesion	7 o' clock	Bulges the capsule with a broad base of attachment	Excellent, no limitations
7	Right peripheral mid gland	9–10 o'clock	Bulges the capsule laterally	Hemorrhage limits sensitivity and functional characterization
8	Left peripheral mid gland	3–5 o'clock	Bulges the capsule, no gross extraprostatic extension	Motion and hemorrhage limit evaluation
9	Left peripheral gland	4 o'clock	Intact, no suspicion for involvement	Excellent, no limitations

Abbreviation: EPE, extraprostatic extension.

Table 3. Pathologic findings determined from post resection whole-mount pathology in nine patients undergoing radical prostatectomy with histologically proven EPE

Case	*Gleason*	*Location of EPE*	*Staging*	*Age*	*PSA*	*Surgical margins at site of EPE*
1	3+4	Right posterior	pT3bNxMx	61	5.8	Negative
2	3+4	Right posterior	pT3aN0Mx	55	2.7	Positive
3	4+5	Right posterior	pT3bpN1Mx	64	8.2	Negative
4	4+3	Right posterior	pT3aN1Mx	64	4.2	Positive
5	4+5	Right posterior	pT3aN1Mx	68	7	Positive
6	4+3	Right posterior	pT3apN0Mx	56	10	Positive
7	4+3	Right antero-lateral	pT3apN0Mx	67	5.1	Negative
8	4+3	Left posterior	pT3aN0Mx	65	5.8	Negative
9	3+4	Right lateral, midline posterior	pT3aN0Mx	53	3.9	Negative

Abbreviation: EPE, extraprostatic extension.

cellularity maps across the patient pool, (ii) subtracting this measured mean value from each subjects RSI cellularity map and (iii) dividing by the measured normal prostate s.d. Correction of image distortions in RSI maps due to B0 field inhomogeneities was performed using the alternating phase-encode technique.[24] As per standard clinical protocol, radiology reports were generated by an experienced radiologist for each of the patients blinded to the RSI results (Table 2).

Correlation of RSI-MRI with histopathology

Whole-mount histopathology was performed on the 28 enrolled patients who underwent RSI-MRI and subsequent radical prostatectomy. For the 10 radical prostatectomy patients with histologically identified EPE (pT3 disease), presurgical pelvic RSI-MRI imaging was reviewed. Out of 10 patients with histologically identified EPE, 1 patient was excluded due to an error in data collection of the MRI-RSI, where distortion correction was unable to be performed. Thus, a total of nine pT3 patients were used for evaluation in this pilot study.

The area of tumor was identified by an experienced uropathologist (Table 3). Clinical images were reviewed in a nonblinded fashion to verify performance of RSI-MRI (Figure 1), where pathology was available for comparison. Standard MRI (including T2, perfusion and traditional DWI), RSI-MRI and histopathology were compared at a multidisciplinary tumor board consisting of radiologists, urologists and uropathologists. RSI-MRI

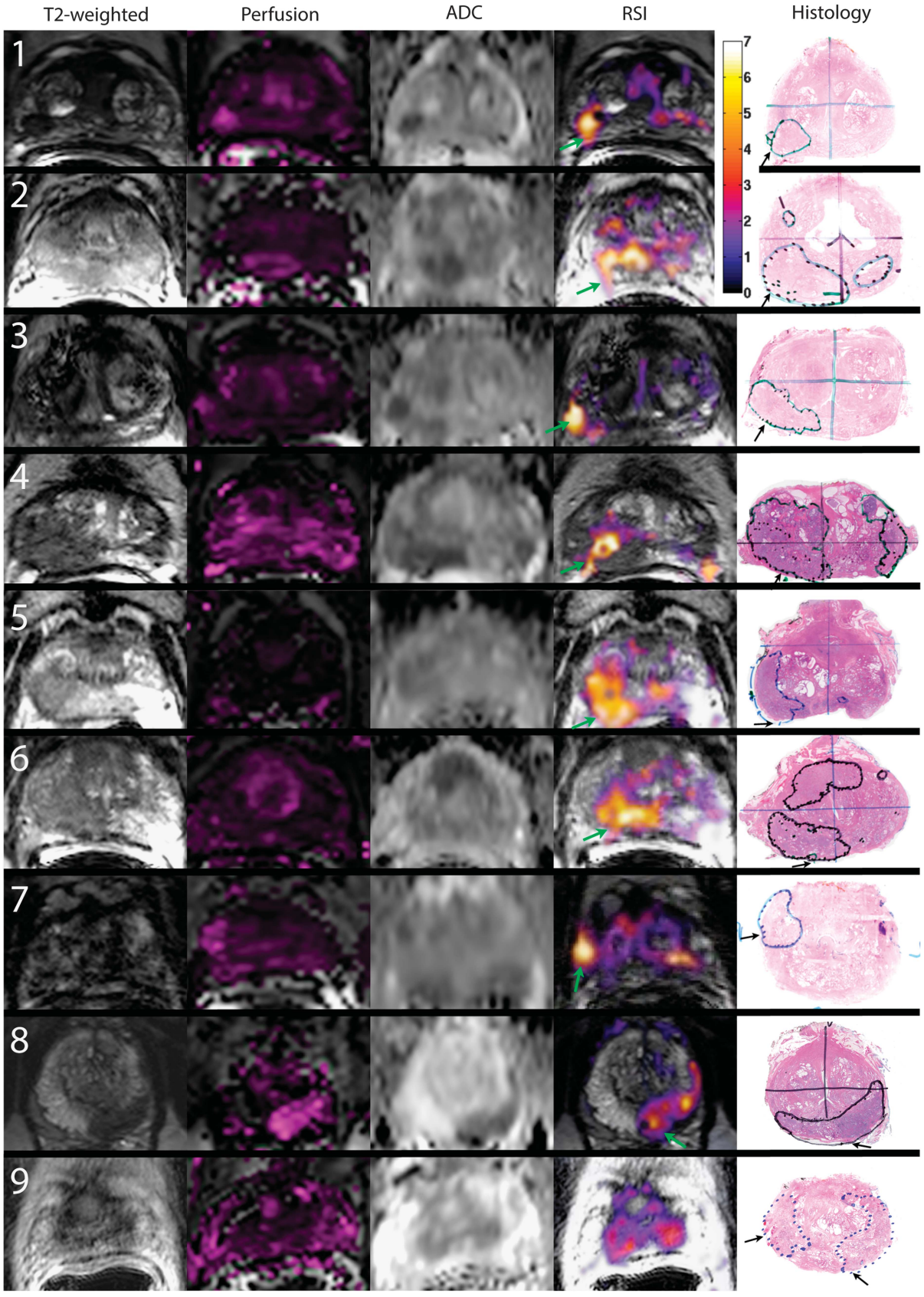

Figure 1. MRI and whole-mount pathology for nine prostate cancer patients with EPE. Column 1: T2-weighted images, column 2: perfusion K_{trans} maps, column 3: standard apparent diffusion coefficient (ADC) maps ($b = 0$, 100, 400 and 800 s mm^{-2}), column 4: RSI *z*-score maps and column 5: whole-mount pathology with tumor and area of EPE identified. Color bar represents *z*-scores from zero to seven for the RSI maps. EPE, extraprostatic extension; MRI, magentic resonance imaging; RSI, restriction spectrum imaging.

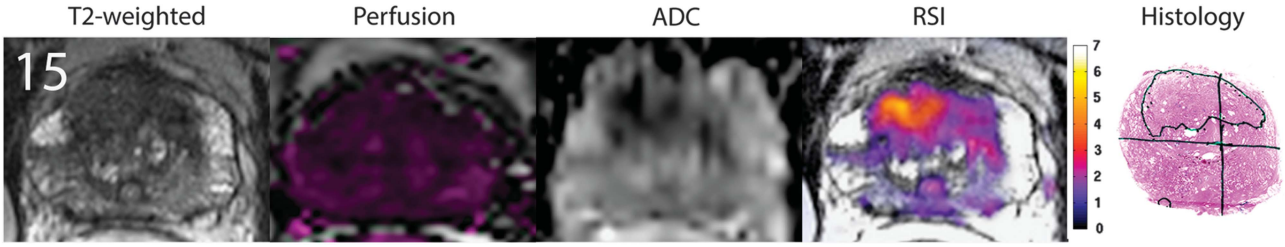

Figure 2. MRI and whole-mount pathology for a representative prostate cancer patient without histologically proven EPE. Column 1: T2-weighted image, column 2: perfusion K_{trans} map, column 3: standard apparent diffusion coefficient (ADC) map ($b = 0$, 100, 400 and 800 s mm^{-2}), column 4: RSI *z*-score map and column 5: whole-mount pathology with tumor and area of EPE identified. Color bar represents *z*-scores from zero to seven for the RSI map. EPE, extraprostatic extension; MRI, magentic resonance imaging; RSI, restriction spectrum imaging.

Table 4. Pathologic findings determined from postresection whole-mount pathology in 18 patients undergoing radical prostatectomy without EPE

Case	*Gleason*	*Staging*	*Age*	*PSA*
10	4+3+5	pT2aN0Mx	62	4.8
11	3+4	pT2NxMx	63	7
12	4+3	pT2cN0Mx	45	6.5
13	3+3	pT2NxMx	71	7.3
14	4+5	pT2N0Mx	62	4.6
15	3+3	pT2cNxMx	59	4.43
16	3+3	pT2N0Mx	61	9.2
17	3+4	pT2cN0Mx	68	6.7
18	3+4	pT2bN0Mx	55	4.7
19	3+4	pT2cNxMx	64	5.8
20	3+4	pT2cN0Mx	61	3.4
21	3+3	pT2cpNxMx	60	6
22	4+3	pT2N0Mx	61	6.6
23	3+4	pT2NxMx	65	5.4
24	3+4	pT2NxMx	50	8.9
25	3+4	pT2aN0Mx	44	2.8
26	3+4	pT2cNxMx	58	3.8
27	3+4	pT2NxMx	53	5.5

Abbreviation: EPE, extraprostatic extension.

images were reviewed to determine if the RSI signal extended beyond the prostatic capsule, defined as the T2-hypointense thin line separating parenchymal tissue from extraprostatic fat and neurovascular structures. RSI maps were spatially corrected and overlayed on standard T2 maps to determine whether the RSI signal was intracapsular or bulging, blurring or grossly extending beyond the capsule. This evaluation was then compared with the preoperative MRI radiology reports to determine whether EPE was suspected without RSI-MRI.

RESULTS

Standard MRI

Using the standard preoperative MR protocol (T1 perfusion, T2 and basic diffusion-weighting), patients 1 and 5 demonstrated radiologic findings consistent with capsular involvement and EPE (Table 2). Patient 4′s imaging findings were suspicious for EPE but not definitive. Patients 3, 6, 7 and 8 demonstrated standard MR radiologic findings consistent with bulging of the capsule, but no indication of EPE. Patient 2′s and patient 9′s standard imaging did not indicate the concern for pathology abutting the capsule.

Restriction spectrum imaging

On analysis of RSI-MRI, eight of nine (89%) patients demonstrated EPE (Figure 1, column 4; Table 3). For eight of the nine patients, the areas of EPE detected on MRI-RSI correlated with the areas encircled on the whole-mount histopathology. Four of eight (50%) patients with RSI-MRI detected EPE also had positive surgical margins. Two patients (one and three, corresponding to Figure 1 and Table 3) had pT3b disease. In patient 1, MRI-RSI demonstrated seminal vesicle involvement. In patient 3, MRI-RSI did not demonstrate any involvement. For patient 9, a patient with histologically proven EPE, MRI-RSI was concerning for tumor bulging the capsule and possible EPE, but not definitively (and considered negative for EPE on MRI-RSI).

Figure 2 demonstrates a representative patient who did not demonstrate EPE on histology or imaging. Table 4 presents the data from the 18 patients without histologically proven EPE. For the 18 non-EPE patients, MRI-RSI detected the histologically proven area of pT2 disease.

DISCUSSION

In this pilot clinical study, we demonstrate the potential for our novel prostate RSI-MRI technique to substantially improve upon current imaging-based modalities for the diagnosis and staging of PCa. In our series, RSI-MRI successfully identified pT3 disease in eight of nine (89%) patients, whereas standard MRI accurately identified only two of nine (22%). These data justify further translational studies of RSI-MRI for PCa detection and staging.

RSI-MRI's sensitivity to intracellular diffusivity differentiates it from standard DWI.[22] Extracellular signal emanating from surrounding inflammatory processes and hemorrhage contributes less to the signal detected by RSI-MRI as compared with standard DWI. RSI-MRI minimizes these effects by focusing on the signal emanating from intracellular tumor cells (restricted diffusion within small spherical compartments), with less focus on the extracellular signal (hindered and free water diffusion). RSI-MRI achieves this by collecting diffusion images over an extended *b*-value range ($b = 0$–4000 s mm^{-2}) and decomposing the relative contribution from separable water compartments within voxels using a linear mixture model framework.[22,23] Standard quantitative diffusion techniques acquire data with *b*-values < 1000 s mm^{-2}. In addition, unlike conventional diffusion imaging and apparent diffusion coefficient maps, RSI-MRI maps are distortion corrected and directly overlayed on T2 anatomic images with voxel specific accuracy, permitting more accurate assessment of signal beyond the capsular border. This increases the conspicuity of the EPE.

Current standard MRI prostate protocols lack accurate localization of PCa. RSI-MRI notably improves tumor localization with MRI, potentially rendering MRI more relevant in a variety of clinical scenarios. Presurgical MRI results may provide additional information for clinicians and patients by informing surgical planning (that is, nerve sparing). Other potential applications for RSI-MRI meriting further study include lesion localization for targeting of image-guided biopsies, serial imaging in an active surveillance population and evaluation of posttreatment recurrence following primary radiotherapy.

A challenge in further developing clinical applications of RSI-MRI lies in accurately defining its specificity, sensitivity and positive and negative predictive values. Limitations of this current study included the small number of patients, and the retrospective nonblinded nature of the study. This was necessary for this pilot study for innovative methodological development, but suffers due to potential reader bias. It is also important to note that, although we have included surgical margin data, the MRI-RSI results did not inform surgical technique.

An ongoing, blinded prospective study will allow for more detailed evaluations of the operating characteristics of RSI-MRI relative to standard MRI and its ability to inform clinical care. RSI-MRI is a standardized quantitative technique and can potentially be employed across platforms and institutions. The color bar in Figure 1 illustrates the *z*-score scale for the RSI maps. As the number of enrollees increase, the *z*-score threshold range for concern for malignancy can be determined by pooling the variance across patients. One of the challenges of standard diffusion imaging, is that the apparent diffusion coefficient values are not standardized across MRI scanners. The *z*-score is a standardized statistical method and inherently normalizes across the patient pool. Thus, the *z*-score is a value that can be compared across different scanners and provides a more robust value for relative comparison.

In summary, in this proof of concept study, we present our initial clinical experience with prostate RSI-MRI. RSI-MRI has the potential to substantially improve the radiological detection and characterization of PCa. Further translational studies will focus on defining its operating characteristics with respect to diagnosis and staging.

CONFLICT OF INTEREST

The authors declare no conflict of interest.

ACKNOWLEDGEMENTS

We would like to thank Brenda Brown for her help on this project. This work was supported by the Department of Defense, Prostate Cancer Research Program W81XWH-13-1-0391, the American Cancer Society—Institutional Research Grant Number 70-002 and the UCSD Clinician Scientist Program.

REFERENCES

1 Turkbey B, Pinto PA, Mani H, Bernardo M, Pang Y, McKinney YL *et al.* Prostate cancer: value of multiparametric MR imaging at 3 T for detection--histopathologic correlation. *Radiology* 2010; **255**: 89–99.
2 Isebaert S, Van den Bergh L, Haustermans K, Joniau S, Lerut E, De Wever L *et al.* Multiparametric MRI for prostate cancer localization in correlation to whole-mount histopathology. *J Magn Reson Imaging* 2013; **37**: 1392–1401.
3 Haider MA, van der Kwast TH, Tanguay J, Evans AJ, Hashmi A-T, Lockwood G *et al.* Combined T2-weighted and diffusion-weighted MRI for localization of prostate cancer. *AJR Am J Roentgenol* 2007; **189**: 323–328.
4 Rastinehad AR, Baccala AA, Chung PH, Proano JM, Kruecker J, Xu S *et al.* D'Amico risk stratification correlates with degree of suspicion of prostate cancer on multiparametric magnetic resonance imaging. *J Urol* 2011; **185**: 815–820.
5 Rais-Bahrami S, Türkbey B, Rastinehad AR, Walton-Diaz A, Hoang AN, Siddiqui MM *et al.* Natural history of small index lesions suspicious for prostate cancer on multiparametric MRI: recommendations for interval imaging follow-up. *Diagn Interv Radiol* 2014; **20**: 293–298.
6 Abd-Alazeez M, Ahmed HU, Arya M, Charman SC, Anastasiadis E, Freeman A *et al.* The accuracy of multiparametric MRI in men with negative biopsy and elevated PSA level--can it rule out clinically significant prostate cancer? *Urol Oncol* 2014; **32**: 45.e17–22.
7 Hoeks CMA, Somford DM, van Oort IM, Vergunst H, Oddens JR, Smits GA *et al.* Value of 3-T multiparametric magnetic resonance imaging and magnetic resonance-guided biopsy for early risk restratification in active surveillance of low-risk prostate cancer: a prospective multicenter cohort study. *Invest Radiol* 2014; **49**: 165–172.
8 Stamatakis L, Siddiqui MM, Nix JW, Logan J, Rais-Bahrami S, Walton-Diaz A *et al.* Accuracy of multiparametric magnetic resonance imaging in confirming eligibility for active surveillance for men with prostate cancer. *Cancer* 2013; **119**: 3359–3366.
9 Abd-Alazeez M, Kirkham A, Ahmed HU, Arya M, Anastasiadis E, Charman SC *et al.* Performance of multiparametric MRI in men at risk of prostate cancer before the first biopsy: a paired validating cohort study using template prostate mapping biopsies as the reference standard. *Prostate Cancer Prostatic Dis* 2014; **17**: 40–46.
10 Turkbey B, Mani H, Aras O, Ho J, Hoang A, Rastinehad AR *et al.* Prostate cancer: can multiparametric MR imaging help identify patients who are candidates for active surveillance? *Radiology* 2013; **268**: 144–152.
11 Rais-Bahrami S, Siddiqui MM, Turkbey B, Stamatakis L, Logan J, Hoang AN *et al.* Utility of multiparametric magnetic resonance imaging suspicion levels for detecting prostate cancer. *J Urol* 2013; **190**: 1721–1727.
12 Park JJ, Kim CK, Park SY, Park BK, Lee HM, Cho SW. Prostate cancer: role of pretreatment multiparametric 3-T MRI in predicting biochemical recurrence after radical prostatectomy. *Am J Radiol* 2014; **202**: W459–W465.
13 Somford DM, Hamoen EH, Fütterer JJ, van Basten JP, Hulsbergen-van de Kaa CA, Vreuls W *et al.* The predictive value of endorectal 3 Tesla multiparametric magnetic resonance imaging for extraprostatic extension in patients with low, intermediate and high risk prostate cancer. *J Urol* 2013; **190**: 1728–1734.
14 Lim HK, Kim JK, Kim KA, Cho K-S. Prostate cancer: apparent diffusion coefficient map with T2-weighted images for detection--a multireader study. *Radiology* 2009; **250**: 145–151.
15 Tanimoto A, Nakashima J, Kohno H, Shinmoto H, Kuribayashi S. Prostate cancer screening: the clinical value of diffusion-weighted imaging and dynamic MR imaging in combination with T2-weighted imaging. *J Magn Reson Imaging* 2007; **25**: 146–152.
16 Donati OF, Jung SI, Vargas HA, Gultekin DH, Zheng J, Moskowitz CS *et al.* Multiparametric prostate MR imaging with T2-weighted, diffusion-weighted, and dynamic contrast-enhanced sequences: are all pulse sequences necessary to detect locally recurrent prostate cancer after radiation therapy? *Radiology* 2013; **268**: 440–450.
17 Mazaheri Y, Hricak H, Fine SW, Akin O, Shukla-Dave A, Ishill NM *et al.* Prostate tumor volume measurement with combined T2-weighted imaging and diffusion-weighted MR: correlation with pathologic tumor volume. *Radiology* 2009; **252**: 449–457.
18 Miao H, Fukatsu H, Ishigaki T. Prostate cancer detection with 3-T MRI: comparison of diffusion-weighted and T2-weighted imaging. *Eur J Radiol* 2007; **61**: 297–302.
19 Giannarini G, Nguyen DP, Thalmann GN, Thoeny HC. Diffusion-weighted magnetic resonance imaging detects local recurrence after radical prostatectomy: initial experience. *Eur Urol* 2012; **61**: 616–620.
20 Donato F, Costa DN, Yuan Q, Rofsky NM, Lenkinski RE, Pedrosa I. Geometric distortion in diffusion-weighted MR imaging of the prostate-contributing factors and strategies for improvement. *Acad Radiol* 2014; **21**: 817–823.
21 Yoshimitsu K, Kiyoshima K, Irie H, Tajima T, Asayama Y, Hirakawa M *et al.* Usefulness of apparent diffusion coefficient map in diagnosing prostate carcinoma: correlation with stepwise histopathology. *J Magn Reson Imaging* 2008; **27**: 132–139.
22 White NS, Leergaard TB, D'Arceuil H, Bjaalie JG, Dale AM. Probing tissue microstructure with restriction spectrum imaging: histological and theoretical validation. *Hum Brain Mapp* 2013; **34**: 327–346.
23 White NS, McDonald CR, Farid N, Kuperman JM, Kesari S, Dale AM. Improved conspicuity and delineation of high-grade primary and metastatic brain tumors using 'restriction spectrum imaging': quantitative comparison with high B-value DWI and ADC. *AJNR Am J Neuroradiol* 2012; **34**: 958–964.
24 Holland D, Kuperman JM, Dale AM. Efficient correction of inhomogeneous static magnetic field-induced distortion in Echo Planar Imaging. *Neuroimage* 2010; **50**: 175–183.
25 White NS, Dale AM. Distinct effects of nuclear volume fraction and cell diameter on high b-value diffusion MRI contrast in tumors. *Magn Reson Med* 2013; **72**: 1435–1443.